On the Capacity of Wireless Powered Communication Systems Over Rician Fading Channels

Feiran Zhao, *Student Member, IEEE*, Hai Lin, *Senior Member, IEEE*, Caijun Zhong, *Senior Member, IEEE*, Zoran Hadzi-Velkov, *Senior Member, IEEE*, George K. Karagiannidis, *Fellow, IEEE*, and Zhaoyang Zhang, *Member, IEEE*

***Abstract*— In this paper, we consider a point-to-point multi-input multi-output wireless-powered communication system, where the source S is powered by a dedicated power beacon (PB) with multiple antennas. Employing the time splitting protocol, the energy constrained source S first harvests energy through the radio-frequency signals sent by the PB and then uses this energy to transmit information to the destination D. Unlike several prior works, we assume that the energy transfer link is subjected to Rician fading, which is a real fading environment, due to relatively short range power transfer distance and the existence of a strong line of sight path. We present a comprehensive analysis of the achievable ergodic capacity in two scenarios, depending on the availability of channel state information (CSI) at PB, namely, the *absence of CSI* and *partial CSI*. For the former case, equal power allocation is used, while for the later one, energy beamforming is used to enhance the energy transfer efficiency. For both the cases, closed-form expressions for the upper and lower bounds of the ergodic capacity are derived. Furthermore, the optimal time split is discussed, and the capacity in the low and high signal-to-noise ratio regimes is studied through simple closed-form expressions. Numerical results and simulations are provided to validate the theoretical analysis. The results show that the Rician factor K has a significant impact on the ergodic capacity performance, and this impact strongly depends on the availability of the CSI at the PB.**

***Index Terms*— Energy harvesting, MIMO, Rician channels, wireless powered communications.**

Manuscript received April 19, 2017; revised July 30, 2017; accepted September 12, 2017. Date of publication September 20, 2017; date of current version January 13, 2018. This work was supported in part by the National Natural Science Foundation of China under Grant 61671406, the Zhejiang Provincial Natural Science Foundation of China (LR15F010001), the National Science and Technology Major Project of China 2017ZX03001002-003. The work of Zoran Hadzi-Velkov was supported in part by the Ministry of Education and Science of Macedonia under Grant 16-4644. The associate editor coordinating the review of this paper and approving it for publication was W. Zhang. *(Corresponding author: Caijun Zhong.)*

F. Zhao, C. Zhong, and Z. Zhang are with the Institute of Information and Communication Engineering, Zhejiang University, Hangzhou 310027, China (e-mail: caijunzhong@zju.edu.cn).

H. Lin is with the Department of Electrical and Information Systems, Osaka Prefecture University, Osaka 599-8531, Japan (e-mail: lin@eis.osakafu-u.ac.jp).

Z. Hadzi-Velkov is with the Faculty of Electrical Engineering and Information Technologies, Ss. Cyril and Methodius University, 1000 Skopje, Macedonia (e-mail: zoranhv@feit.ukim.edu.mk).

G. K. Karagiannidis is with the Department of Electrical and Computer Engineering, Aristotle University of Thessaloniki, 54 124 Thessaloniki, Greece (e-mail: geokarag@auth.gr).

Color versions of one or more of the figures in this paper are available online at http://ieeexplore.ieee.org.

Digital Object Identifier 10.1109/TCOMM.2017.2754488

I. Introduction

PROVIDING reliable and efficient energy supply for energy constrained devices in wireless communication networks has now become an important issue. For instance, mobile phones and various type of sensors are typically powered by batteries that have limited operation time, which requires either to be frequently plugged into the power grid for recharging or periodical battery replacement, thereby incurring high costs as well as greatly affecting the user experience. Responding to this, harvesting energy from ambient environment such as solar and wind has been proposed in [1] and [2]. Nevertheless, due to the instability and the inherent randomness of nature resources, it is extremely challenging to produce a stable energy output required for communication systems, with strict quality-of-service constraints.

A. Literature

Recently, with the advance of wireless power transfer (WPT) technology, radio frequency (RF) signals based energy harvesting has received considerable attention [3]. In addition, because RF signals can be fully controlled, and thus, it allows great flexibility, compared with ambient resources. Leveraging on the fact that RF signals can carry both information and energy, a new paradigm, referred to as simultaneous wireless information and power transfer (SWIPT) has emerged [4]. The fundamental tradeoff between the information transmission and energy harvesting for SWIPT systems have been studied in the pioneering works of Varshney [5] and Grover and Sahai [6]. Later in [7], practical architectures for SWIPT systems were proposed, and the optimal transmit covariance achieving the rate-energy region were characterized. In order to improve the rate-energy region, more sophisticated architectures were proposed in [8] and [9]. In the meantime, the impact of imperfect CSI on the performance of SWIPT systems was investigated in [10]. Moreover, the application of SWIPT in cooperative relaying systems was investigated in [11]–[18].

All these prior works adopts the hybrid base station (BS) model, where the BS acts both as energy and information source. However, due to the fact that the operational sensitivity level of the information decoder (in the order of -100 dBm) differs substantially from that of the energy harvester (in the

order of -10 dBm), the hybrid BS model can only power mobile users within a very short range (say, less than 10 meters) [19], which makes the full network coverage for SWIPT impractical. In order to address this issue, the authors of [20] proposed a new network architecture, where a dedicated power beacon (PB) is introduced in the network to power the wireless devices. Since then, significant research efforts has been devoted to understand the performance of PB-assisted systems. More specifically, in [21], the optimal resource allocation problem of a PB-assisted wireless powered communication (WPC) network was investigated, while the authors in [22] studied the maximum achievable throughput of a wireless powered cooperative relaying network, where both user and relay were powered by a dedicated PB. Later in [23], a novel adaptive transmission scheme that improves the system throughput, was proposed for a PB-assisted buffer-aided cooperative relaying system. Furthermore, the authors in [24] investigated the average throughput of a point-to-point single-input single-output WPC network powered by a dedicated PB, where it was shown that the employment of multiple antennas at the PB have a positive impact on the average throughput.

B. Motivation and Contribution

Unlike most of the aforementioned papers that assume the Rayleigh fading channels for both energy and information transfer links, the authors in [25] studied the optimal design of channel training for MIMO WET systems in Rician fading channels. In practice, due to the relatively short power transfer distance, the line-of-sight (LOS) path is very likely to exist between the PB and the energy harvesting node. Therefore the Rician fading distribution is the most appropriate model for the WPT link, and it is of great significance to study the achievable performance of WPC systems operating over Rician fading channels. Specifically, we consider a point-to-point MIMO communication link powered by a dedicated PB, and we assume Rician fading channels for the WPT link. Furthermore, we consider the time splitting protocol, i.e., the transmitter first harvests energy from the PB, and then uses the harvested energy to transmit information to the receiver. Under this consideration, we investigate the achievable ergodic capacity performance in two different scenarios depending on the available CSI at the PB, namely, absence of CSI, and partial CSI at PB. Specifically, for both cases, we present closed-from expressions for the upper and lower bound of the ergodic capacity. Based on these expressions, the optimal time split is also studied. In addition, we look into the high and low SNR regimes, and present simple and concise expressions for key performance measures such as high SNR slope, power offset and minimum required energy per information bit, which reveals the impact of key system parameters on the ergodic capacity of the system. The findings of the paper suggests that the Rician factor K has a significant impact on the system performance, and a large K is desirable. Moreover, the impact of Rician factor K on the ergodic capacity depends on the available CSI at the PB.

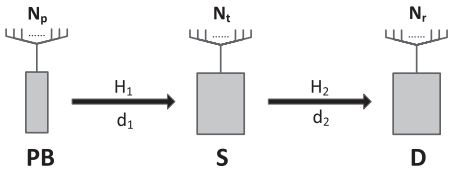

Fig. 1. System model.

C. Structure and Notations

The rest of the paper is organized as follows. Section II provides the system model, while section III gives some preliminary results, which will be invoked in the following analysis. Section IV investigates the capacity performance when no CSI is available at PB, and section V discusses the capacity performance when partial CSI is available at PB. Numerical results and simulations are provided in section VI. Finally, section VII concludes the paper with some remarks.

Notation: We use bold upper case and lower case letters to represent matrices and vectors, respectively, while lower case letters represents the scalars. Also, $||\cdot||$ stands for the Frobenius norm, $\mathrm{E}(\cdot)$ denotes the expectation of a random variable, the symbol $\dagger$ is the conjugate transpose operator, $\det(\cdot)$ represents the determinant of a matrix, $\mathcal{CN}(\cdot)$ means complex Gaussian distribution and $\mathrm{tr}(\cdot)$ is the trace operator for matrix.

II. System Model

We consider a point to point WPC system where an energy constrained source S communicates with a destination D, as depicted in Fig.1. It is assumed that S does not have external energy supply, and is powered by a dedicated PB.[1] The PB is equipped with N_p antennas, while S and D are equipped with N_t and N_r antennas, respectively. Due to significant path loss, current WPT technique is suitable for relatively short range energy transfer. Hence, a LOS path is very likely to exist between PB and S, and the Rician distribution can be used to model the channel $\mathbf{H}_1$ between PB and S, namely

$$\mathbf{H}_1 = \sqrt{\frac{K}{K+1}}\mathbf{H_0} + \sqrt{\frac{1}{K+1}}\mathbf{H}_w, \tag{1}$$

where K is the Rician factor, and $\mathbf{H}_w \in \mathbb{C}^{N_t \times N_p}$ is the channel matrix with entries being independent and identically distributed (i.i.d.) circularly symmetric Gaussian random variables (RVs), i.e., $\mathbf{H}_w$ has $\mathcal{CN}(0,1)$ entries, while $\mathbf{H}_0 \in \mathbb{C}^{N_t \times N_p}$ is a full rank deterministic matrix, normalized such that $||\mathbf{H}_0||^2 = N_p N_t$. On the other hand, Rayleigh distribution is adopted to model the information transmission channel $\mathbf{H}_2$ between S and D, i.e., the entries of $\mathbf{H}_2$ are i.i.d. $\mathcal{CN}(0,1)$ RVs.

As in [24], we consider the time splitting protocol. Hence, an entire transmission block of length T is split into two separate phases. In the first phase of duration τT $(0 < \tau < 1)$, S harvests energy from PB. In the second phase, S transmits information to D using the harvested energy.

[1]Similar as in [24], we assume that the transmitter S is solely powered via RF energy harvesting. The utilization of multiple antennas at PB and S guarantee the high energy harvesting efficiency [27], [28]. Hence S can harvest enough energy to support its own power requirements.

A. Energy Harvesting

During the EH phase, we consider two different scenarios depending on the type of available CSI at PB, namely, the absence of CSI case, and the partial CSI case. Note that when no CSI is available at PB, equal power allocation is used at the PB, hence, the performance gain by deploying multiple antennas at PB is insignificant. Nevertheless, the results of no CSI case serve as a useful performance benchmark when quantifying the performance gain due to partial CSI at PB.

1) Absence of CSI at PB: When no CSI is available, the transmit power is equally distributed among each antenna at PB. Hence, the received signals at S is given by

$$\mathbf{y}_s = \sqrt{\frac{\phi P_b}{d_1^l N_p}}\mathbf{H}_1\mathbf{s} + \mathbf{n}_s, \tag{2}$$

where P_b is the transmit power of PB, d_1 is the distance between PB and S, l denotes the path-loss exponent, $\mathbf{s} \in \mathbb{C}^{N_p \times 1}$ is the normalized energy signal transmitted by PB, which satisfies $\mathrm{E}\{\mathbf{s}\mathbf{s}^\dagger\} = \mathbf{I}_{N_p}$, while $\mathbf{n}_s \in \mathbb{C}^{N_t \times 1}$ is the zero mean additive white Gaussian noise (AWGN) at S, satisfying $\mathrm{E}\{\mathbf{n}_s\mathbf{n}_s^\dagger\} = N_0\mathbf{I}_{N_t}$. In addition, ϕ represents the path-loss normalization factor, which is defined as $\phi = s_0/d_0^{-l}$ where d_0 is a reference distance in meter and s_0 is the propagation loss factor measured at d_0 [26]. Hence, at the end of the first phase, the harvested energy at S can be computed as

$$E_h = \frac{\eta\tau T\phi P_b}{d_1^l N_p}\mathrm{tr}\{\mathbf{H}_1\mathbf{H}_1^\dagger\}, \tag{3}$$

where $0 < \eta < 1$ denotes the energy conversion efficiency.

2) Partial CSI at PB: In practice, instantaneous CSI of H_1 can be difficult to acquire. However, it is relatively easy to obtain statistical CSI, such as the mean of the channel. As such, we consider the scenario where the mean channel of $\mathbf{H}_1$, $\mathbf{H}_0$, is available at PB, and energy beamforming can be performed to improve the energy transfer efficiency during the power transfer phase. Hence, the received signal at S can be written as

$$\mathbf{y}_s = \sqrt{\frac{\phi P_b}{d_1^l}}\mathbf{H}_1\mathbf{w}_p x + \mathbf{n}_s, \tag{4}$$

where $\mathbf{w}_p$ is the energy beamforming vector satisfying $||\mathbf{w}_p||_2^2 = 1$, and x is the normalized signal satisfying $\mathrm{E}\{|x|^2\} = 1$. Using the notations $\alpha = \sqrt{K/(K+1)}$ and $\beta = \sqrt{1/(K+1)}$, (4) can be rewritten as

$$\mathbf{y}_s = \sqrt{\frac{\phi P_b}{d_1^l}}\alpha\mathbf{H}_0\mathbf{w}_p x + \sqrt{\frac{\phi P_b}{d_1^l}}\beta\mathbf{H}_w\mathbf{w}_p x + \mathbf{n}_s. \tag{5}$$

Due to the fact that PB is aware of the mean matrix $\mathbf{H}_0$, the beamforming vector $\mathbf{w}_p$ is chosen to be the eigenvector associated with the largest eigenvalue of matrix $\mathbf{H}_0{}^\dagger\mathbf{H}_0$. Therefore the harvested energy at S is given by

$$E_h = \frac{\eta\tau T\phi P_b}{d_1^l}\left(\alpha^2\lambda_1 + \beta^2||\mathbf{H}_w\mathbf{w}_p||_2^2\right), \tag{6}$$

where λ_1 represents the largest eigenvalue of $\mathbf{H}_0^\dagger\mathbf{H}_0$.

B. Information Transfer

In the remaining time of duration $(1-\tau)T$, S transmits information to D using the all the energy harvested during the WPT phase.[2] As we mainly focus on understanding the impact of the line-of-sight effect in the WPT phase on the ergodic capacity, we assume that no CSI is available at S but perfect CSI at D during the IT phase in order to simplify the analysis. Hence, equal power allocation is adopted at S and the received signal at D is given by

$$\mathbf{y}_d = \sqrt{\frac{\phi P_s}{d_2^l N_t}}\mathbf{H}_2\mathbf{x} + \mathbf{n}_d, \tag{7}$$

where d_2 is the distance between S and D. $\mathbf{x} \in \mathbb{C}^{N_t \times 1}$ indicates the normalized signal vector with $\mathrm{E}\{\mathbf{x}\mathbf{x}^\dagger\} = \mathbf{I}_{N_t}$, $\mathbf{n}_d \in \mathbb{C}^{N_r \times 1}$ is the AWGN at D satisfying $\mathrm{E}\{\mathbf{n}_d\mathbf{n}_d{}^\dagger\} = N_0\mathbf{I}_{N_r}$. The transmit power at S is given by

$$P_s = \frac{E_h}{(1-\tau)T}. \tag{8}$$

and the total transmit SNR at S is defined as

$$\gamma_t = \frac{P_s}{N_0}. \tag{9}$$

C. Ergodic Capacity

Assuming no CSI is available at S but perfect CSI at D, the ergodic capacity can be expressed as [30]

$$C = (1-\tau)\mathrm{E}\left\{\log_2\det\left(\mathbf{I}_{N_r} + \frac{\phi\gamma_t}{d_2^l N_t}\mathbf{H}_2\mathbf{H}_2^\dagger\right)\right\}. \tag{10}$$

Considering that the transmit power of S comes from the energy harvesting phase, we define the system SNR as

$$\rho = \frac{P_b}{N_0}. \tag{11}$$

III. Prelimimaries

In this section, we provide a statistical framework, which is used later for the performance analysis of the considered system.

Proposition 1: The RV, $A_1 = \mathrm{tr}\{\mathbf{H}_1\mathbf{H}_1{}^\dagger\}$, follows noncentral chi-square distribution with probability density function (PDF) given by

$$\begin{aligned} f_{A_1}(x) &= (K+1)\left(\frac{2(K+1)x}{\theta}\right)^{\frac{N_pN_t-1}{2}} \\ &\times I_{N_pN_t-1}\left(\sqrt{2(K+1)\theta x}\right)\exp\left(-(K+1)x - \frac{\theta}{2}\right), \end{aligned} \tag{12}$$

where $I_a(z)$ denotes the Bessel function of the first kind. The degree of freedom and the noncentral parameter of A_1 are $2N_pN_t$ and $\theta = 2KN_pN_t$, respectively.

[2] In this paper, we have assumed that the power consumption at the transmit/receive antenna circuitry at S is negligible, compared to that for the information transmission. This can be easily justified since [9] mentioned that as the transmission distance gets large, the transmission power becomes the dominant power consumption of the transmitter. Besides, same assumptions have been widely made in WPC literatures [24], [29].

Proof: From (1), it can be concluded that the elements of matrix $\mathbf{H}_1$ are complex Gaussian RVs with nonzero mean. Therefore, the trace of the matrix $\mathbf{H}_1\mathbf{H}_1{}^\dagger$, which equals the quadratic sum of $2N_pN_t$ such RVs, is a noncentral chi-square RV. This completes the proof. ∎

Lemma 1: Some moments of the RV A_1 are given by

$$\mathrm{E}\{A_1\} = N_pN_t, \tag{13}$$

$$\mathrm{E}\{A_1^2\} = \frac{N_pN_t\left((1+2K)(N_pN_t+1)+K^2N_pN_t\right)}{(K+1)^2}, \tag{14}$$

$$\mathrm{E}\{A_1^{i-n}\} = \frac{\exp\left(-\frac{\theta}{2}\right)\Gamma(N_pN_t+i-n)}{\Gamma(N_pN_t)(K+1)^{i-n}} \times\Phi\left(N_pN_t+i-n, N_pN_t, \frac{\theta}{2}\right), \tag{15}$$

where $n = \min(N_t, N_r)$, $i = \{0, 1, 2\ldots n\}$, and $\Phi(x, y, z)$ denotes the Kummer confluent hypergeometric function [32].

Proof: By using the PDF of A_1 in (12) and utilizing [32, eqs. (8.406) and (6.631)], (13)–(15) can be easily obtained. ∎

Lemma 2: The expected logarithm of A_1 is given by

$$\begin{aligned}&\mathrm{E}\{\ln A_1\}\\ &= \sum_{r=1}^{N_pN_t-1}\left(-\frac{2}{\theta}\right)^r\left(\exp\left(-\frac{\theta}{2}\right)(r-1)! - \frac{(N_pN_t-1)!}{r(N_pN_t-1-r)!}\right)\\ &\quad + \ln\frac{\theta}{2} - \mathrm{E_i}\left(-\frac{\theta}{2}\right) - \ln(K+1),\end{aligned} \tag{16}$$

where $\mathrm{E_i}(x) = \int_{-\infty}^{x}\frac{e^{-t}}{t}dt$ denotes the exponential integral function.

Proof: This lemma can be proved by using the PDF of A_1 in (12) and following the same procedure as in [33, Appendix X]. ∎

Proposition 2: The PDF of the RV, $A_2 = \alpha^2\lambda_1 + \beta^2||\mathbf{H}_w\mathbf{w}_p||_2^2$, is given by

$$f_{A_2}(x) = \frac{(x-\alpha^2\lambda_1)^{N_t-1}}{\Gamma(N_t)\beta^{2N_t}}\exp\left(-\frac{x-\alpha^2\lambda_1}{\beta^2}\right). \tag{17}$$

Proof: According to [42], $|\mathbf{h}_i{}^\dagger\mathbf{w}_p|^2$ follows an exponential distribution with parameter 1, where $\mathbf{h}_i$ is an arbitrary row vector of $\mathbf{H}_w$. Thus, we can deduce that $||\mathbf{H}_w\mathbf{w}_p||_2^2$ is a gamma RV. After some algebraic manipulations, (17) can be proved. ∎

Lemma 3: Some moments of A_2 are given by

$$\mathrm{E}\{A_2\} = \beta^2N_t + \alpha^2\lambda_1, \kappa \tag{18}$$

$$\mathrm{E}\{A_2^2\} = (\beta^2N_t + \alpha^2\lambda_1)^2 + \beta^4N_t, \tag{19}$$

$$\mathrm{E}\{A_2^{i-n}\} = \frac{\exp\left(\frac{\alpha^2\lambda_1}{\beta^2}\right)}{\Gamma(N_t)}\sum_{r=0}^{N_t-1}\binom{N_t-1}{r}(-\alpha^2\lambda_1)^r \times\beta^{2(i-r-n)}\Gamma\left(N_t-r-n+i, \frac{\alpha^2\lambda_1}{\beta^2}\right), \tag{20}$$

where $i = \{0, 1, 2\ldots n\}$.

Proof: Exploiting the PDF of A_2 in (17) and using the integration formula [32, eqs. (3.351) and (3.381)], (18)–(20) can be easily derived. ∎

Lemma 4: The expected logarithm of A_2 is given by

$$\begin{aligned}&\mathrm{E}\{\ln A_2\}\\ &= \ln(\alpha^2\lambda_1) + \sum_{u=0}^{N_t-1}\frac{1}{(N_t-1-u)!}\\ &\quad\times\left(\sum_{k=1}^{N_t-1-u}(k-1)!\left(\frac{-\alpha^2\lambda_1}{\beta^2}\right)^{N_t-1-u-k}\right.\\ &\quad\left.-\left(\frac{-\alpha^2\lambda_1}{\beta^2}\right)^{N_t-1-u}\exp\left(\frac{\alpha^2\lambda_1}{\beta^2}\right)\mathrm{E_i}\left(\frac{-\alpha^2\lambda_1}{\beta^2}\right)\right).\end{aligned} \tag{21}$$

Proof: The result can be obtained with the help of the integration formula [32, eqs. (4.337) and (3.381)]. ∎

IV. Capacity Analysis When CSI Is Not Available

This section presents a detailed study of the system ergodic capacity, assuming that CSI is not available at PB. Due to the involvement of zonal polynomial [31], an exact analysis of the ergodic capacity appears extremely challenging. Therefore we mainly focus on the capacity bounds and its behavior in both high and low SNR regimes.

In this case, the ergodic capacity (10) can be further expressed as

$$C_1(\rho) = (1-\tau)\mathrm{E}\left\{\log_2\det\left(\mathbf{I}_n + \frac{\rho}{N_t}ab_1A_1\mathbf{W}\}\right)\right\}, \tag{22}$$

where $A_1 = \mathrm{tr}\{\mathbf{H}_1\mathbf{H}_1^\dagger\}$, $a = \frac{\tau}{1-\tau}$, $b_1 = \frac{\eta\phi^2}{N_pd_1^ld_2^l}$ and $\mathbf{W}\in\mathbb{C}^{n\times n}$ is the Wishart matrix which equals $\mathbf{H}_2\mathbf{H}_2^\dagger$ when $N_r \le N_t$, or $\mathbf{H}_2^\dagger\mathbf{H}_2$ when $N_r > N_t$. Note that $m = \max\{N_t, N_r\}$.

A. Upper Bound

The following Theorem provides an upper bound to the ergodic capacity.

Theorem 1: The ergodic capacity upper bound is expressed in closed-form as (23) on the top of the next page.

Proof: See Appendix A. ∎

B. Lower Bound

Next, we derive the closed-form expression of the capacity lower bound. In addition, the optimal time split that maximizes the system performance is also obtained in closed-form.

Theorem 2: The ergodic capacity of the system is lower bounded by

$$\begin{aligned}&C_{lb1}(\rho)\\ &= n(1-\tau)\log_2\left(1+\frac{\rho ab_1\theta}{2N_t(K+1)}\exp\left(-\gamma-1\right.\right.\\ &\quad+\sum_{i=1}^{m-n}\frac{1}{i}+\frac{m}{n}\sum_{i=m-n+1}^{m}\frac{1}{i}+\sum_{r=1}^{N_pN_t-1}\left(-\frac{2}{\theta}\right)^r\left(\exp\left(-\frac{\theta}{2}\right)\right.\\ &\quad\left.\left.\left.\times(r-1)! - \frac{(N_pN_t-1)!}{r(N_pN_t-1-r)!}\right) - \mathrm{E_i}\left(-\frac{\theta}{2}\right)\right)\right),\end{aligned} \tag{24}$$

where γ denotes the Euler's constant [30].

Proof: As in [38], we can apply Minkowski's inequality and Jensen's inequality successively to (22) to obtain the

$$C_{ub1}(\rho) = (1-\tau)\left(n\log_2\frac{\rho a b_1}{N_t} + \frac{n}{\ln 2}\left(\ln\frac{\theta}{2(K+1)} - \mathrm{E_i}\left(-\frac{\theta}{2}\right) + \sum_{r=1}^{N_pN_t-1}\left(-\frac{2}{\theta}\right)^r\left(\exp\left(-\frac{\theta}{2}\right)(r-1)! - \frac{(N_pN_t-1)!}{r(N_pN_t-1-r)!}\right)\right)\right.$$
$$\left. + \log_2\left(\frac{\exp\left(-\frac{\theta}{2}\right)m!}{\Gamma(N_pN_t)}\sum_{i=0}^{n}\frac{\binom{n}{i}\Phi(N_pN_t+i-n, N_pN_t, \frac{\theta}{2})\Gamma(N_pN_t+i-n)}{(m-i)!}\times\left(\frac{\rho a b_1}{N_t(K+1)}\right)^{i-n}\right)\right). \quad (23)$$

following inequality

$$C_1(\rho) \geq n(1-\tau) \times \log_2\left(1+\exp\left(\mathrm{E}\left\{\ln\left(\frac{\rho a b_1 A_1}{N_t}(\det\mathbf{W})^{\frac{1}{n}}\right)\right\}\right)\right). \quad (25)$$

Then, noticing that the random variables A_1 and $\mathbf{W}$ are independent, we have

$$\mathrm{E}\left\{\ln\left(\frac{\rho a b_1 A_1}{N_t}(\det\mathbf{W}^{\frac{1}{n}})\right)\right\} = \ln\left(\frac{\rho a b_1}{N_t}\right) + \mathrm{E}\{\ln A_1\} + \frac{1}{n}\mathrm{E}\{\ln\det\mathbf{W}\}. \quad (26)$$

The last term in (26) can be computed according to [30, Appendix B]. Next, invoking *Lemma 2*, the desired result can be obtained after some algebraic manipulations. ■

Similarly, in order to gain the optimal time split τ_{lb1}^* for the lower bound, we have the following optimization problem

$$\tau_{lb1}^* = \arg\max_{\tau} C_{lb1}(\tau) \quad \text{s.t. } 0<\tau<1. \quad (27)$$

where C_{lb1} is the lower bound with respect to τ, which can be expressed in compact form as

$$C_{lb1}(\tau) = n(1-\tau)\log_2\left(1+c_1\frac{\tau}{1-\tau}\right). \quad (28)$$

Note that c_1 in (28) is a value, that does not involve τ, and is given by

$$c_1 = \frac{\rho b_1\theta}{2N_t(K+1)}\exp\left(-\gamma - 1 - \mathrm{E_i}\left(-\frac{\theta}{2}\right) + \sum_{i=1}^{m-n}\frac{1}{i} + \frac{m}{n}\sum_{i=m-n+1}^{m}\frac{1}{i} + \sum_{r=1}^{N_pN_t-1}\left(-\frac{2}{\theta}\right)^r\left(\exp\left(-\frac{\theta}{2}\right)(r-1)! - \frac{(N_pN_t-1)!}{r(N_pN_t-1-r)!}\right)\right). \quad (29)$$

Fortunately, the optimization problem above could been solved analytically. Hence, we have the following corollary.

Corollary 1: The optimal time split τ_{lb1}^* for the capacity lower bound is given by

$$\tau_{lb1}^* = \frac{\exp\left(\mathrm{W}\left(\frac{c_1-1}{e}\right)+1\right)-1}{\exp\left(\mathrm{W}\left(\frac{c_1-1}{e}\right)+1\right)-1+c_1}, \quad (30)$$

where $\mathrm{W}(\cdot)$ denotes the Lambert W function [34] and e stands for the base of natural logarithm.

Proof: The desired result can be obtained by using [24, Lemma 3]. ■

C. High SNR Regime

In this section, we investigate the capacity behavior of the considered WPC system in the high SNR regime. Firstly, we characterize the high SNR approximation for the ergodic capacity in (22), and then discuss the optimal time split.

1) High SNR Approximation: At high SNRs, it was proved that the ergodic mutual information, namely the ergodic capacity, of a wireless MIMO communication system behave as [30]

$$\mathcal{C}(\rho) = S_\infty\left(\log_2\rho - L_\infty\right) + o(1). \quad (31)$$

The notations S_∞ and L_∞ are key performance measures that dictate the capacity behavior at high SNRs, and are defined as below:

The capacity slope S_∞ in bit/s/Hz/3 dB, is given by

$$S_\infty = \lim_{\rho\to\infty}\frac{C(\rho)}{\log_2\rho}, \quad (32)$$

while the quantity L_∞ in (31), which denotes the power offset that anchors the capacity expansion, is given by

$$L_\infty = \lim_{\rho\to\infty}\left(\log_2\rho - \frac{C(\rho)}{S_\infty}\right) \quad (33)$$

in 3 dB units. Note that this performance measure was first introduced in [37].

Capitalizing on the capacity expression in (22), we obtain the following theorem.

Theorem 3: The key parameters that dominate the capacity behavior in the high SNR regime is given by

$$L_\infty = -\frac{1}{\ln 2}\left(\ln\frac{ab_1\theta}{2N_t(K+1)} + \sum_{r=1}^{N_pN_t-1}\left(-\frac{2}{\theta}\right)^r \times\left(\exp\left(-\frac{\theta}{2}\right)(r-1)! - \frac{(N_pN_t-1)!}{r(N_pN_t-1-r)!}\right) + \sum_{i=1}^{m-n}\frac{1}{i} + \frac{m}{n}\sum_{i=m-n+1}^{m}\frac{1}{i} - \mathrm{E_i}\left(-\frac{\theta}{2}\right) - \gamma - 1\right), \quad (34)$$

and

$$S_\infty = n(1-\tau). \quad (35)$$

Proof: See Appendix B. ■

Theorem 3 indicates that the high SNR slope S_∞ scales linearly with n, as in the conventional point-to-point MIMO systems with constant energy supply [30]. However, the difference is that the high SNR slope S_∞ is also limited by the time splitting parameter, τ.

Substituting (34) and (35) into (31), we derive the final expression for the capacity approximation of the considered WPC system in the high SNR regime as

$$C_{h_1}(\rho) = \frac{n(1-\tau)}{\ln 2}\left(\ln\frac{\rho a b_1 \theta}{2N_t(K+1)} + \sum_{r=1}^{N_pN_t-1}\left(-\frac{2}{\theta}\right)^r \times\left(\exp\left(-\frac{\theta}{2}\right)(r-1)! - \frac{(N_pN_t-1)!}{r(N_pN_t-1-r)!}\right) + \sum_{i=1}^{m-n}\frac{1}{i} + \frac{m}{n}\sum_{i=m-n+1}^{m}\frac{1}{i} - \mathrm{E_i}\left(-\frac{\theta}{2}\right) - \gamma - 1\right). \tag{36}$$

2) Optimal Time Split at High SNRs: Similarly, the expression of $C_{h_1}(\rho)$ in (36) can also be regarded as a function of the time split, τ, given the specific system SNR, ρ. Thus, we have

$$C_{h_1}(\tau) = n(1-\tau)\left(\log_2\frac{\tau}{1-\tau} + c_2\right), \tag{37}$$

where the term c_2 in the above equation stands for a constant value, which is irrelevant to the time split τ. This term is defined as

$$c_2 = \frac{1}{\ln 2}\left(\ln\frac{\rho b_1\theta}{2N_t(K+1)} + \sum_{r=1}^{N_pN_t-1}\left(-\frac{2}{\theta}\right)^r \times\left(\exp\left(-\frac{\theta}{2}\right)(r-1)! - \frac{(N_pN_t-1)!}{r(N_pN_t-1-r)!}\right) + \sum_{i=1}^{m-n}\frac{1}{i} + \frac{m}{n}\sum_{i=m-n+1}^{m}\frac{1}{i} - \mathrm{E_i}\left(-\frac{\theta}{2}\right) - \gamma - 1\right). \tag{38}$$

Based on (37), the optimal time split could be obtained by solving the following optimization

$$\tau_{h_1}^* = \arg\max_{\tau} C_{h_1}(\tau) \quad \text{s.t. } 0 < \tau < 1. \tag{39}$$

Note that since the above optimization problem maximizes the capacity approximation in the high SNR regime, the solution $\tau_{h_1}^*$ can be regarded as an approximation of the optimal time split that maximizes the exact system ergodic capacity at high SNRs. Therefore, such optimization problem is of great significance.

The optimization problem in (39) could be solved analytically. Thus we have the following result:

Corollary 2: The optimal time split $\tau_{h_1}^*$ that maximizes the capacity of the considered wireless powered communication system in the high SNR regime is given by

$$\tau_{h_1}^* = \frac{\exp\left(\mathrm{W}\left(\exp\left(c_2\ln 2 - 1\right)\right) - c_2\ln 2 + 1\right)}{1 + \exp\left(\mathrm{W}\left(\exp\left(c_2\ln 2 - 1\right)\right) - c_2\ln 2 + 1\right)}. \tag{40}$$

Proof: See [24, *Lemma 4*]. ∎

D. Low SNR Regime

In this section, we study the capacity performance of the considered WPC system in the low SNR regime. Similarly, we first characterize the low SNR approximation of the ergodic capacity in (22), and then investigate the optimal time split.

1) Low SNR Approximation: In the low SNR regime, it is useful to investigate the capacity, in terms of the normalized transmit energy per information bit, E_b/N_0, rather than the system SNR, ρ. The key performance measures at low SNRs are thus E_b/N_{0min}, i.e., the minimum energy per information bit required to convey any positive rate reliably, and S_0, the capacity slope therein in bit/s/Hz/(3-dB)). Using these two parameters, the capacity of wireless powered multi-antenna communication system can be well approximated by [35]

$$C\left(\frac{E_b}{N_0}\right) \approx S_0\log_2\left(\frac{\frac{E_b}{N_0}}{\frac{E_b}{N_{0\,min}}}\right). \tag{41}$$

Considering the fact that the transmit power at S is originated from the radio frequency signals emitted by PB, in the following context, we define $\frac{E_b}{N_0}$ to be the normalized energy per-information bit required from PB. Therefore, we have

$$\frac{E_b}{N_0} = \frac{P_s}{N_0}\frac{1}{C(\rho)} = \frac{\rho}{C(\rho)}. \tag{42}$$

With the definition above, the key performance measures that dictate the capacity behavior in the low SNR regime can be obtained from $C(\rho)$ via [36]

$$\frac{E_b}{N_{0\,min}} = \frac{1}{\dot{C}(0)}, \tag{43}$$

$$S_0 = -\frac{2\left[\dot{C}(0)\right]^2}{\ddot{C}(0)}\ln 2, \tag{44}$$

where $\dot{C}(\cdot)$ and $\ddot{C}(\cdot)$ denote the first and second order derivatives taken with respect to ρ, respectively.

Theorem 4: The key performance measures in low SNR regime, namely the minimum energy per information bit required from PB and the capacity slope are given by

$$\frac{E_b}{N_{0\,min}} = \frac{d_1^l d_2^l \ln 2}{\tau\eta\phi^2 N_t N_r}, \tag{45}$$

$$S_0 = \frac{2(1-\tau)(K+1)^2 N_p N_r N_t^2}{(N_t+N_r)\left((2K+1)(N_pN_t+1)+K^2N_pN_t\right)}. \tag{46}$$

Proof: See Appendix C. ∎

Substituting (45) and (46) into (41) yields the closed-form expression of the system capacity in the low SNR regime,

$$C_{l_1}\left(\frac{E_b}{N_0}\right) = \frac{2(1-\tau)(K+1)^2 N_p N_t^2 N_r}{(N_t+N_r)\left((2K+1)(N_pN_t+1)+K^2N_pN_t\right)} \times\log_2\left(\frac{\tau\eta\phi^2 N_t N_r}{d_1^l d_2^l\ln 2}\times\frac{E_b}{N_0}\right). \tag{47}$$

Remark 1: From (45), we can readily observe that the minimum energy per information is a decreasing function with respect to N_t and N_r, respectively, which intuitively means that more energy can be captured with more antennas at the both the transmitter and the receiver side. Besides, as can be observed from (46), the low SNR slope is an increasing function of N_p, N_t and N_r, respectively, which indicates the benefit of deploying multiple antennas at the PB, S and D.

2) Optimal Time Split at Low SNRs: We now study the optimal time split τ. In the low SNR regime, the capacity can be approximated by

$$C_{l_1}(\tau) = c_3(1-\tau)\log_2(c_4\tau), \tag{48}$$

where c_3 and c_4 are constants and given by

$$c_3 = \frac{2(K+1)^2 N_p N_t^2 N_r}{(N_t+N_r)((2K+1)(N_pN_t+1)+K^2N_pN_t)}, \tag{49}$$

$$c_4 = \left(\frac{E_b}{N_0}\right)\frac{\eta\phi^2 N_t N_r}{d_1^l d_2^l \ln 2}. \tag{50}$$

Thus, the optimal time split τ could be obtained by solving the following optimization

$$\begin{aligned}\tau_{l_1}^* &= \arg\max_{\tau} C_{l_1}(\tau)\\ &\text{s.t. } 0<\tau<1.\end{aligned} \tag{51}$$

Note that solving the above optimization problem improves the capacity performance for WPC systems that operating in the low SNR regime. Similarly, the above optimization could be solved analytically, and we have the following result:

Corollary 3: The optimal time split $\tau_{l_1}^*$ that maximizes the capacity of the considered WPC system at low SNRs is given by

$$\tau_{l_1}^* = \exp\left(\mathrm{W}\left(\exp\left(1+\ln c_4\right)\right) - \ln c_4 - 1\right). \tag{52}$$

Proof: Taking the first derivative of $C_{l_1}(\tau)$ with respect to τ and set $\frac{dC_{l_1}(\tau)}{d\tau}=0$, we have

$$\ln(c_4\tau) = \frac{1}{\tau} - 1. \tag{53}$$

Inspired by [24], and after some algebraic manipulations, we can rewrite the last equation as

$$\begin{aligned}&\ln\left(\tau\exp\left(1+\ln c_4\right)\right)\exp\left(\ln\left(\tau\exp\left(1+\ln c_4\right)\right)\right)\\ &\qquad = \exp\left(1+\ln c_4\right),\end{aligned} \tag{54}$$

which is in the form of the standard definition of lambert W function. This completes the proof. ∎

Remark 2: According to (30) and (40), the Rician factor K is required for the optimization of time split. Since the Rician factor K varies slowly, it can be obtained at the PB via feedback with low cost.

V. Capacity Analysis With Partial CSI

When partial CSI is available at PB, the ergodic capacity in (10) can be rewritten as

$$C_2(\rho) = (1-\tau)\mathrm{E}\left\{\log_2\det\left(\mathbf{I}_n + \frac{\rho}{N_t}ab_2A_2\mathbf{W}\right)\right\}, \tag{55}$$

where $b_2 = \frac{\eta\phi^2}{d_1^l d_2^l}$ and $A_2 = \alpha^2\lambda_1 + \beta^2||\mathbf{H}_w\mathbf{w}_p||_2^2$.

A. Upper Bound

The following Theorem provides an upper bound to the ergodic capacity.

Theorem 5: The ergodic capacity upper bound is expressed in closed-form as (56) on the bottom of this page.

Proof: Following the same steps in Appendix A, and invoking *Lemma 3* and *Lemma 4*, (56) can be obtained. ∎

B. Lower Bound

Theorem 6: The capacity is lower bounded by

$$\begin{aligned}&C_{lb2}(\rho)\\ &= n(1-\tau)\log_2\Bigg(1+\frac{\rho ab_2}{N_t}\exp\Bigg(\sum_{i=1}^{m-n}\frac{1}{i}+\frac{m}{n}\\ &\quad\times\sum_{i=m-n+1}^{m}\frac{1}{i}-1-\gamma+\sum_{u=0}^{N_t-1}\frac{1}{(N_t-1-u)!}\Bigg(\sum_{k=1}^{N_t-1-u}(k-1)!\\ &\quad\times\left(\frac{-\alpha\lambda_1}{\beta^2}\right)^{N_t-1-u-k} - \exp\left(\frac{\alpha^2\lambda_1}{\beta^2}\right)\mathrm{E_i}\left(\frac{-\alpha^2\lambda_1}{\beta^2}\right)\\ &\quad\times\left(\frac{-\alpha^2\lambda_1}{\beta^2}\right)^{N_t-1-u}\Bigg)+\ln(\alpha^2\lambda_1)\Bigg)\Bigg)\end{aligned} \tag{57}$$

Proof: Applying Minkowski's inequality and Jensen's inequality successively to (55), and invoking *Lemma 4* yields the desired result.

The lower bound in (57) can be regarded as a function of τ, given some fixed system SNR ρ. Thus, we formulate the following optimization problem in order to obtain the optimal time split τ_{lb2}^* that maximizes the capacity lower bound.

$$\begin{aligned}\tau_{lb2}^* &= \arg\max_{\tau} C_{lb2}(\tau)\\ &\text{s.t. } 0<\tau<1,\end{aligned} \tag{58}$$

The lower bound with respect to τ can be written in the compact form as

$$C_{lb2}(\tau) = n(1-\tau)\log_2\left(1+c_5\frac{\tau}{1-\tau}\right). \tag{59}$$

$$\begin{aligned}C_{ub2}(\rho) = (1-\tau)\Bigg(&\log_2\Bigg(\frac{\exp\left(\frac{\alpha^2\lambda_1}{\beta^2}\right)}{\beta^{2N_t}\Gamma(N_t)}\sum_{i=0}^{n}\sum_{r=0}^{N_t-1}\left(\frac{\rho ab_2}{N_t}\right)^{i-n}\binom{N_t-1}{r}(-\alpha^2\lambda_1)^r\beta^{2(N_t-r-n+i)}\\ &\times\Gamma\left(N_t-r-n+i,\frac{\alpha^2\lambda_1}{\beta^2}\right)\binom{n}{i}\frac{m!}{(m-i)!}\Bigg)+n\log_2\left(\frac{\rho ab_2\alpha^2\lambda_1}{N_t}\right)+\frac{n}{\ln 2}\Bigg(\sum_{u=0}^{N_t-1}\frac{1}{(N_t-1-u)!}\\ &\times\Bigg(\sum_{k=1}^{N_t-1-u}(k-1)!\left(\frac{-\alpha^2\lambda_1}{\beta^2}\right)^{N_t-1-u-k} - \exp\left(\frac{\alpha^2\lambda_1}{\beta^2}\right)\mathrm{E_i}\left(\frac{-\alpha^2\lambda_1}{\beta^2}\right)\left(\frac{-\alpha^2\lambda_1}{\beta^2}\right)^{N_t-1-u}\Bigg)\Bigg)\Bigg).\end{aligned} \tag{56}$$

where c_5 is given by

$$c_5 = \frac{\rho b_2}{N_t}\exp\Bigg(\ln(\alpha^2\lambda_1) + \sum_{i=1}^{m-n}\frac{1}{i} + \frac{m}{n}\sum_{i=m-n+1}^{m}\frac{1}{i} - 1 - \gamma + \sum_{u=0}^{N_t-1}\frac{1}{(N_t-1-u)!}\times\Bigg(\sum_{k=1}^{N_t-1-u}(k-1)! \times \left(\frac{-\alpha\lambda_1}{\beta^2}\right)^{N_t-1-u-k} - \exp\left(\frac{\alpha^2\lambda_1}{\beta^2}\right)\mathrm{E_i}\left(\frac{-\alpha^2\lambda_1}{\beta^2}\right) \times \left(\frac{-\alpha^2\lambda_1}{\beta^2}\right)^{N_t-1-u}\Bigg)\Bigg). \quad (60)$$

Notice that (59) is in the same form as (28). Therefore, referring to the solution of the optimization problem in (27), we can obtain the solution of the above problem in the following corollary.

Corollary 4: The optimal time split τ^*_{lb2} for the capacity lower bound is given by

$$\tau^*_{lb2} = \frac{\exp\left(\mathrm{W}\left(\frac{c_5-1}{e}\right)+1\right)-1}{\exp\left(\mathrm{W}\left(\frac{c_5-1}{e}\right)+1\right)-1+c_5}. \quad (61)$$

C. High SNR Regime

1) High SNR Approximation: At high SNRs, the capacity behavior of the partial CSI case can also be characterized by (31). According to (32) and (33), we have the following result.

Theorem 7: In the high SNR regime, the high SNR slope of the system is given by

$$S_\infty = n(1-\tau), \quad (62)$$

while the power offset is given by

$$L_\infty = \log_2\frac{N_t}{ab_2} - \frac{1}{\ln 2}\left(\sum_{i=1}^{m-n}\frac{1}{i} + \frac{m}{n}\sum_{i=m-n+1}^{m}\frac{1}{i} - \gamma - 1\right) - \frac{1}{\ln 2}\Bigg(\ln(\alpha^2\lambda_1) + \sum_{u=0}^{N_t-1}\frac{1}{(N_t-1-u)!} \times \Bigg(\sum_{k=1}^{N_t-1-u}(k-1)!\left(\frac{-\alpha^2\lambda_1}{\beta^2}\right)^{N_t-1-u-k} - \exp\left(\frac{\alpha^2\lambda_1}{\beta^2}\right) \times \mathrm{E_i}\left(\frac{-\alpha^2\lambda_1}{\beta^2}\right)\left(\frac{-\alpha^2\lambda_1}{\beta^2}\right)^{N_t-1-u}\Bigg)\Bigg). \quad (63)$$

Proof: Following the same steps in Appendix B, and utilizing *Lemma 4*, we have the desired result. ∎

By substituting the two performance measures above into (31), the high SNR approximation of the system capacity can be expressed as

$$C_{h_2}(\rho) = \frac{n(1-\tau)}{\ln 2}\Bigg(\ln\frac{\rho a b_2\alpha^2\lambda_1}{N_t} + \sum_{i=1}^{m-n}\frac{1}{i} + \frac{m}{n} \times \sum_{i=m-n+1}^{m}\frac{1}{i} - \gamma - 1 + \sum_{u=0}^{N_t-1}\frac{1}{(N_t-1-u)!}\Bigg(\sum_{k=1}^{N_t-1-u}(k-1)! \times \left(\frac{-\alpha^2\lambda_1}{\beta^2}\right)^{N_t-1-u-k} - \exp\left(\frac{\alpha^2\lambda_1}{\beta^2}\right) \times \mathrm{E_i}\left(\frac{-\alpha^2\lambda_1}{\beta^2}\right)\left(\frac{-\alpha^2\lambda_1}{\beta^2}\right)^{N_t-1-u}\Bigg)\Bigg). \quad (64)$$

2) Optimal Time Split: After some algebraic manipulations, (64) can be rewritten as a function with respect to τ:

$$C_{h_2}(\tau) = n(1-\tau)\left(\log_2\frac{\tau}{1-\tau} + c_6\right), \quad (65)$$

where c_6 denotes the constant component, that does not involve τ, and is given by

$$c_6 = \frac{1}{\ln 2}\Bigg(\ln\frac{\rho b_2\alpha^2\lambda_1}{N_t} + \frac{1}{\ln 2}\Bigg(\sum_{i=1}^{m-n}\frac{1}{i} + \frac{m}{n}\sum_{i=m-n+1}^{m}\frac{1}{i} - \gamma - 1\Bigg) + \sum_{u=0}^{N_t-1}\frac{1}{(N_t-1-u)!}\times\Bigg(\sum_{k=1}^{N_t-1-u}(k-1)! \times \left(\frac{-\alpha^2\lambda_1}{\beta^2}\right)^{N_t-1-u-k} - \exp\left(\frac{\alpha^2\lambda_1}{\beta^2}\right)\mathrm{E_i}\left(\frac{-\alpha^2\lambda_1}{\beta^2}\right) \times \left(\frac{-\alpha^2\lambda_1}{\beta^2}\right)^{N_t-1-u}\Bigg)\Bigg). \quad (66)$$

Based on (65), we have the following optimization problem

$$\tau^*_{h_2} = \arg\max_{\tau} C_{h_2}(\tau) \quad \text{s.t. } 0 < \tau < 1. \quad (67)$$

Due to the fact that (65) is in the same form with (37), the solution for the above optimization problem can be given in the following corollary directly.

Corollary 5: The optimal time split that maximizes the system capacity in high SNR regime is given by

$$\tau^*_{h_2} = \frac{\exp\left(\mathrm{W}(\exp\left(c_6\ln 2 - 1\right)) - c_6\ln 2 + 1\right)}{1+\exp\left(\mathrm{W}(\exp\left(c_6\ln 2 - 1\right)) - c_6\ln 2 + 1\right)}. \quad (68)$$

D. Low SNR Regime

1) Low SNR Approximation: Capitalizing on the ergodic capacity expression in (55), we have the following theorem.

Theorem 8: At low SNRs, the key performance measures for the system capacity are given by

$$S_0 = \frac{2N_tN_r(1-\tau)}{(N_t+N_r)\left(1+\frac{N_t}{(N_t+K\lambda_1)^2}\right)}, \quad (69)$$

and

$$\frac{E_b}{N_{0\,min}} = \frac{d_1^l d_2^l \ln 2}{\tau\eta\phi^2 N_r(\beta^2 N_t + \alpha^2\lambda_1)}. \quad (70)$$

Substituting (69) and (70) into (41), we have the closed form approximation for the capacity in low SNR regime as

$$C_{l_2}\left(\frac{E_b}{N_0}\right) = \frac{2N_tN_r(1-\tau)}{(N_t+N_r)\left(1+\frac{N_t}{(N_t+K\lambda_1)^2}\right)} \times \log_2\left(\frac{E_b}{N_0}\cdot\frac{\tau\eta N_r\phi^2(\beta^2N_t+\alpha^2\lambda_1)}{d_1^l d_2^l\ln 2}\right). \quad (71)$$

Remark 3: From (69) and (70), it is observed that S_0 is an increasing function with respect to N_r, and $E_b/N_{0_{min}}$ is a decreasing function with respect to N_r, indicating double benefits of increasing N_r. Furthermore, it is easy to see that S_0 is an increasing function of K. As for the impact of K on $E_b/N_{0_{min}}$, we observe from (70) that K affects $E_b/N_{0_{min}}$ only through the term $\beta^2 N_t + \alpha^2 \lambda_1$. It can be shown that the sign of the first derivative of $1/(\beta^2 N_t + \alpha^2 \lambda_1)$ with respect to K depends on $\nabla = N_t - \lambda_1$. Since $||\mathbf{H}_0||^2 = N_p N_t$, it is not difficult to show that $\nabla < 0$, implying that $E_b/N_{0_{min}}$ is a decreasing function of K.

2) Optimal Time Split: The low SNR approximation in (71) can also be regarded as a function of τ. Therefore we have

$$C_{l_2}(\tau) = c_7(1-\tau)\log_2(c_8\tau). \tag{72}$$

Note that c_7 and c_8 are both irrelevant to τ, given the specific $\frac{E_b}{N_0}$, and are given by

$$c_7 = \frac{2N_tN_r}{(N_t+N_r)\left(1+\frac{N_t}{(N_t+K\lambda_1)^2}\right)}, \tag{73}$$

$$c_8 = \frac{E_b}{N_0}\cdot\frac{\eta N_r\phi^2(\beta^2N_t+\alpha^2\lambda_1)}{d_1^l d_2^l \ln 2}. \tag{74}$$

Thus, to characterize the optimal time split that maximizes the capacity approximation in low SNR regime, we have the following optimization problem

$$\begin{aligned}\tau_{l_2}^* = &\arg\max_{\tau} C_{l_2}(\tau)\\ &\text{s.t. } 0<\tau<1.\end{aligned} \tag{75}$$

Once again, due to the fact that (72) and (48) are in the same form, the solution for the above problem could be obtained directly. And we have the next corollary.

Corollary 6: The optimal time split that maximizes the system capacity in low SNR regime is given by

$$\tau_{l_2}^* = \exp\left(\mathrm{W}(\exp(1+\ln c_8)) - \ln c_8 - 1\right). \tag{76}$$

Remark 4: According to (61), (68) and (76), the Rician factor K and λ_1 are required for the optimization of time split. Since the PB have access to the statistical CSI, no additional overhead is required.

VI. Numerical Results and Simulations

In this section, we provide numerical results and simulations to validate the analytical expressions presented in the previous sections, and investigate the impact of key system parameters on the system performance. Throughout this section, unless otherwise specified, we adopt the following set of parameters: The time split for EH and IT is chosen to be 0.5, while the distances d_1 and d_2 are set to be 7 and 15 meters, respectively. The path loss exponent l is set to be 2.5. Furthermore, the energy conversion efficiency η is set to be 0.4. For the channel $\mathbf{H}_1$, we choose the Rician factor $K = 3+\sqrt{12}$ [24]. All the simulation results are obtained by averaging over 10^6 independent trials.

Fig. 2 illustrates the ergodic capacity performance of the considered WPC system with different type of CSI at the PB.

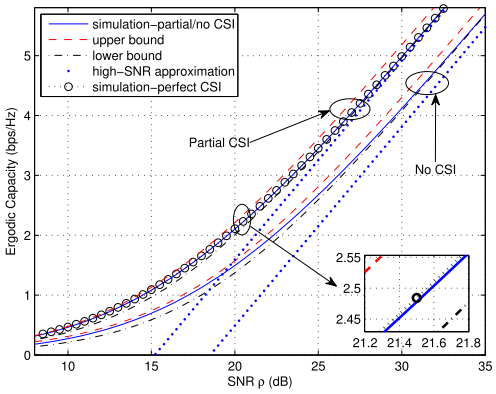

Fig. 2. Ergodic capacity comparison with $N_t = 4$, $N_r = 2$, $N_p = 2$.

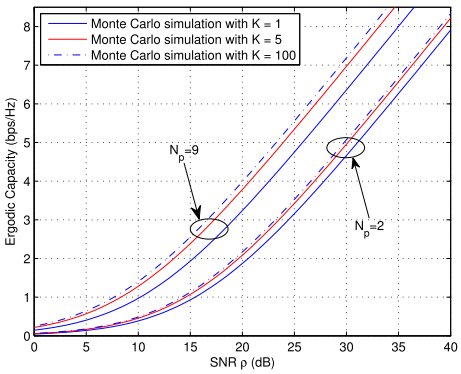

Fig. 3. Impact of K on the ergodic capacity with partial CSI at PB when $N_t = 4$ and $N_r = 2$.

It can be readily observed that, for both cases, the proposed upper bound for the ergodic capacity is reasonably accurate, especially in the low SNR regime, and the lower bound is also very tight, especially in the high SNR regime, where it almost overlaps with the exact curves. Moreover, the achievable ergodic capacity of the system with partial CSI is strictly higher than that of the system with no CSI. This is rather intuitive, since with partial CSI at the PB, energy beamforming can be applied to improve the energy transfer efficiency, which increases the amount of harvested power at S. Furthermore, the performance gap between the partial CSI case and the perfect CSI case is rather insignificant. Since the statistical CSI is much easier to acquire, partial CSI based energy beamforming is of practical interest.

Fig.3 illustrates the impact of the Rician factor K on the system ergodic capacity with partial CSI at PB for different N_p. Intuitively, increasing the number of antennas at PB results in higher ergodic capacity. Also, as can be readily observed, a large K leads to higher capacity, which indicates that a strong LOS path is beneficial in terms of ergodic capacity. Moreover, the capacity gain by increasing the Rician factor K is more significant when N_p is large.

Fig. 4 investigates the impact of the antenna numbers at S and PB on the system capacity with statistical CSI at PB. We observe that the slope of all curves is the same, which is determined by $n = \min(N_t, N_r)$, as expected. Also, adding more antennas at S and PB has a positive impact on the system capacity due to improved energy transfer efficiency and higher array gain.

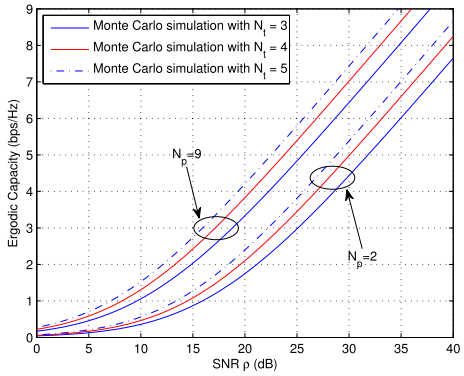

Fig. 4. Impact of N_t on the high SNR approximation with statistical CSI at PB when $N_r = 2$ and $N_p = 2$.

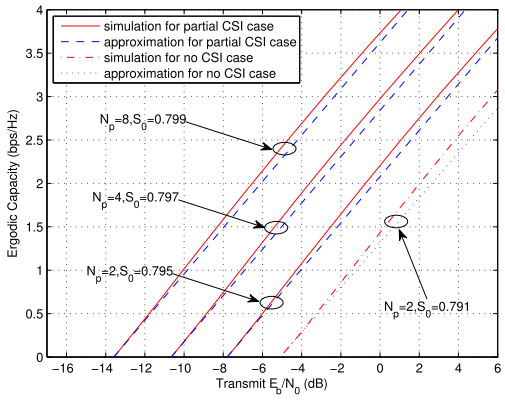

Fig. 5. Low SNR capacity approximation when $N_t = 4$ and $N_r = 2$.

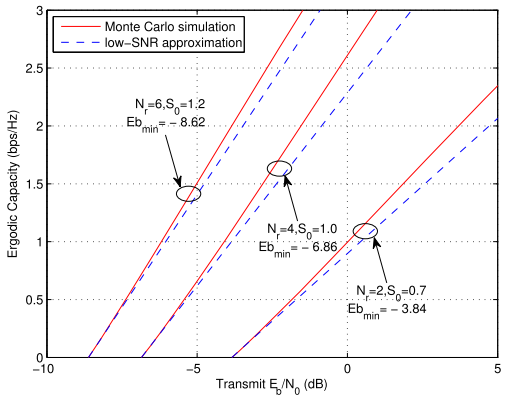

Fig. 6. Low SNR capacity approximation for different N_r with $N_p = 3$, $N_t = 3$, $d_1 = 1$ and $d_2 = 2$.

Fig. 5 shows the capacity performance in the low SNR regime with different N_p for both CSI scenarios. Intuitively, we observe that the ergodic capacity with statistical CSI outperforms the case without CSI, by reducing the minimum energy per information bit required. In addition, for the statistical CSI case, we observe that increasing N_p offers two-fold benefits, i.e., reducing the minimum energy per information required and increasing the low SNR capacity slope. However, the improvement of the low SNR capacity slope is rather insignificant.

Fig. 6 examines the influence of antenna numbers at destination on the system capacity performance at low SNRs when CSI is not available. We observe that the capacity

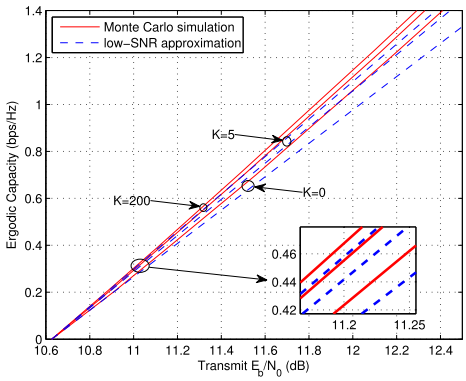

Fig. 7. Impact of Rician factor K on the ergodic capacity without CSI at PB.

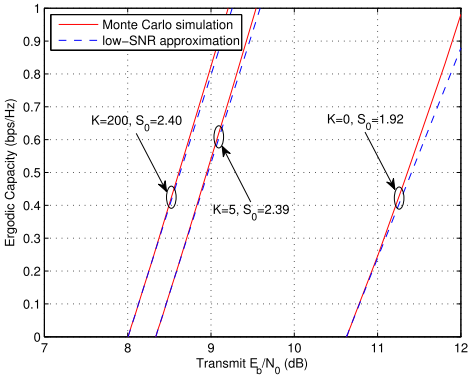

Fig. 8. Impact of Rician factor K on the ergodic capacity with partial CSI at PB.

approximation according to (47) is very accurate for low transmit E_b/N_0 levels. Besides, as illustrated in the figure, increasing N_r helps to reduce the minimum required energy per information bit E_b/N_{0min}, which is in agreement with our analysis in (45). In addition, it is shown that as N_r increases, the low SNR capacity slope S_0 also increases, which confirms the double benefits of adding more antennas at D. It is also worthy pointing out that the benefit of increasing N_r is most significant when N_r is small.

Fig. 7 illustrates the impact of Rician factor K on the low SNR capacity when CSI is not available at PB. From the figure we can observe that the Rician factor K only affects the capacity performance through the low SNR slope, rather than E_b/N_{0min}, as predicated in Theorem.4. In particular, the low SNR slope increases as K becomes larger. However, the improvement becomes insignificant when K is large enough, i.e., $K > 10$.

Fig. 8 investigates the impact of Rician factor K on the low SNR capacity when statistical CSI is available for energy beamforming. It can be readily observed, different from the no CSI case, K affects both the low SNR slope S_0 and E_b/N_{0min}, indicating that the benefit of ling-of-sight effect is more significant if CSI is available at the PB. Similarly, we observe that the benefits become less substantial when K is large enough, i.e., $K > 5$, especially the gain on the low SNR slope.

Fig. 9 examines the optimal time splits that maximize the system capacity in the low SNR regime. The capacity curves were obtained through the low SNR capacity approximations

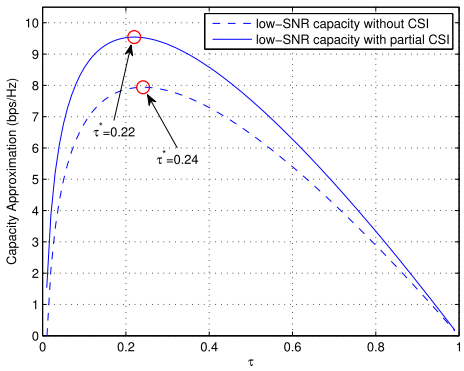

Fig. 9. Optimal time split for low SNR capacity approximation.

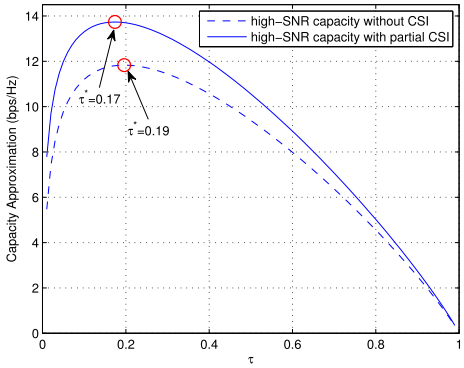

Fig. 10. Optimal time split for high SNR capacity expansion.

in (47) and (71), with respect to the time split τ. While the red circle represents the analytical capacity values given the optimal time splits in (52) and (76). It can be readily observed that the red circle coincides with the maximum value of the corresponding curve, which validates the correctness of the analytical expressions.

Fig. 10 investigates the optimal time splits that maximize the system capacity in high SNR regime. From both figures, it is observed that the system performance with statistical CSI outperforms the case without CSI. In addition, the optimal time split with statistical CSI is always less than that without CSI. This is rather intuitive because when statistical CSI is available, energy beamforming is applied which achieves higher energy transfer efficiency.

VII. Conclusion

We have investigated the capacity behavior of a MIMO WPC system under two different power transfer schemes. In both cases, closed-form expressions for the lower bound and the upper bound of the ergodic capacity are derived. The exact solutions for the optimal time split maximizing the lower bound is obtained. In addition, we studied the capacity behavior under two SNR cases, namely, the high SNR regime and the low SNR regime, where we derived the closed-form approximations of the ergodic capacity for both cases, respectively. Besides, the optimal time split achieving the maximum capacity under these two SNR levels are examined, and exact solutions were obtained. Numerical results and simulations have verified our theoretical analysis. The findings suggest that the WPT process does not affect the capacity slope in high SNR regime, i.e., the capacity slope of the considered WPC system only depends on the minimum antenna number of the information transfer link. However, adding more antennas at PB will improve the system capacity. In addition to that, the optimal time split maximizing the capacity diminishes as the antenna numbers at PB increases, for both high SNR regime and low SNR regime. It is also observed that the larger the Rician factor K, the better quality the approximation of the ergodic capacity. For the two considered power transfer schemes, the numerical results shows the great advantage of utilizing the CSI available at the transmitter side. Future work can be considered when having the instantaneous CSI at PB side.

Appendix A
Proof of Theorem 1

After some algebraic manipulations we can rewrite the capacity expression in (22) as

$$C_1(\rho) = (1-\tau)\left(n\log_2\frac{\rho a b_1}{N_t} + \frac{n}{\ln 2}\mathrm{E}\{\ln A_1\} + \mathrm{E}\left\{\log_2\det\left(\frac{N_t}{\rho a b_1 A_1}\mathbf{I}_n + \mathbf{W}\right)\right\}\right). \quad (77)$$

Note that the last term of the above equation is in the form of a log function, which is concave. Therefore we can apply Jensen's inequality [39] to it and obtain

$$g(\rho) \le \log_2\left(\mathrm{E}\left\{\det\left(\frac{N_t}{\rho a b_1 A_1}\mathbf{I}_n + \mathbf{W}\right)\right\}\right), \quad (78)$$

where $g(\rho)$ is a representative of the last expectation in (77). Next, following the same procedure as [40, *Th. 4*], we can rewrite (78) as

$$g(\rho) \le \log_2\left(\sum_{i=0}^{n}\left(\left(\frac{\rho}{N_t}ab_1\right)^{i-n}\mathrm{E}\left\{A_1^{i-n}\right\}\right) \times \sum_{\substack{\alpha_i\subseteq\{1,2,\ldots,n\}\\ |\alpha_i|=i}}\mathrm{E}\left\{\det\mathbf{W}_{\alpha_i}\right\}\right), \quad (79)$$

where $\mathbf{W}_{\alpha_i}$ is the submatrix formed from $\mathbf{W}$ by deleting rows and columns not indexed by the elements of α_i for $\alpha_i \subseteq \{1,2,\ldots,n\}$. Invoking *Lemma 1* and *Lemma 2*, we obtain the expectation of A_1^{i-n} and $\ln A_1$, respectively. From [41, *Lemma A.1*], we know that the moment of $\det\mathbf{W}$, where $\mathbf{W}\sim\mathcal{W}(m,n)$ is a Wishart matrix, is given by

$$\mathrm{E}\{\det\mathbf{W}\} = \frac{n!}{(n-m)!}. \quad (80)$$

Thus, the last expectation in (79) is obtained. Finally, combining these results yields the closed form expression for the capacity upper bound.

Appendix B
Proof of Theorem 3

First we introduce the derivation of the high SNR slope. Substituting (22) into (32) and after some manipulations,

we have

$$S_\infty = n(1-\tau) + (1-\tau)\lim_{\rho\to\infty}\frac{\mathrm{E}\left\{\log_2\det\left(\frac{ab_1A_1}{N_t}\mathbf{W}\right)\right\}}{\log_2\rho}. \tag{81}$$

Note that in the second term of last equation, the denominator tends to infinity as ρ tends to infinity, while the numerator is bounded. Thus, the second term in (81) is zero and we have the high SNR capacity slope as

$$S_\infty = n(1-\tau). \tag{82}$$

Substituting both (22) and (35) into (33), we can write the power offset as

$$L_\infty = \lim_{\rho\to\infty}\left(\log_2\rho - \frac{1}{n}\mathrm{E}\left\{\log_2\left(\rho^n \times \det\left(\frac{1}{\rho}\mathbf{I}_n + \frac{ab_1A_1}{N_t}\mathbf{W}\right)\right)\right\}\right). \tag{83}$$

Utilizing the independence between A and $\mathbf{W}$, the last equation can be rewritten as

$$L_\infty = \log_2\frac{N_t}{ab_1} - \frac{1}{\ln 2}\mathrm{E}\{\ln A_1\} - \frac{1}{n\ln 2}\mathrm{E}\{\ln\det\mathbf{W}\}. \tag{84}$$

Invoking *Lemma 2*, we have the second term in (84), while the last term in (84) can be derived according to [30, Appendix B]. Finally, combining these results yields the closed form expression of L_∞.

APPENDIX C
PROOF OF THEOREM 4

From (43) and (44), it can be easily observed that the computation of the key performance measures in low SNR regime requires the first- and second- order derivatives of $C_1(\rho)$. To that end, first we introduce the following properties of the determinant of a square matrix $\mathbf{A}$ [35]

$$\frac{d}{du}\ln\det(\mathbf{I}+u\mathbf{A})\,|_{u=0} = \mathrm{tr}(\mathbf{A}), \tag{85}$$

$$\frac{d^2}{du^2}\ln\det(\mathbf{I}+u\mathbf{A})\,|_{u=0} = -\mathrm{tr}(\mathbf{A}^2), \tag{86}$$

Then, substituting (22) into (85) and (86), respectively, we have

$$\dot{C}(0) = \frac{ab_1}{N_t\ln 2}(1-\tau)\mathrm{E}\{A_1\}\mathrm{E}\{\mathrm{tr}(\mathbf{W})\}, \tag{87}$$

$$\ddot{C}(0) = -\frac{\tau^2 b_1^2}{\ln 2(1-\tau)N_t^2}\mathrm{E}\left\{A_1^2\right\}\mathrm{E}\left\{\mathrm{tr}(\mathbf{W}^2)\right\}. \tag{88}$$

The trace of a Wishart matrix can be derived according to [36, *Lemma 4*]. And by invoking *Lemma 1* the expectations in the above equations can be obtained. Thus we get

$$\dot{C}(0) = \frac{\tau b_1 N_p N_t N_r}{\ln 2}, \tag{89}$$

$$\ddot{C}(0) = -\frac{\tau^2 b_1^2 N_p N_r (N_t+N_r)\left((1+2K)(N_pN_t+1)+K^2N_pN_t\right)}{(1-\tau)(K+1)^2\ln 2}. \tag{90}$$

Finally, substituting (89) and (90) into (43) and (44), the key performance measures in the low SNR regime of the considered WPC system can be obtained.

REFERENCES

[1] B. Medepally and N. B. Mehta, "Voluntary energy harvesting relays and selection in cooperative wireless networks," *IEEE Trans. Wireless Commun.*, vol. 9, no. 11, pp. 3543–3553, Nov. 2010.

[2] V. Raghunathan, S. Ganeriwal, and M. Srivastava, "Emerging techniques for long lived wireless sensor networks," *IEEE Commun. Mag.*, vol. 44, no. 4, pp. 108–114, Apr. 2006.

[3] Y. Zeng, B. Clerckx, and R. Zhang, "Communications and signals design for wireless power transmission," *IEEE Trans. Commun.*, vol. 65, no. 5, pp. 2264–2290, May 2017.

[4] Z. Ding *et al.*, "Application of smart antenna technologies in simultaneous wireless information and power transfer," *IEEE Commun. Mag.*, vol. 53, no. 4, pp. 86–93, Apr. 2015.

[5] L. R. Varshney, "Transporting information and energy simultaneously," in *Proc. IEEE ISIT*, Toronto, ON, Canada, Jul. 2008, pp. 1612–1616.

[6] P. Grover and A. Sahai, "Shannon meets Tesla: Wireless information and power transfer," in *Proc. IEEE ISIT*, Austin, TX, USA, Jun. 2010, pp. 2363–2367.

[7] R. Zhang and C. K. Ho, "MIMO broadcasting for simultaneous wireless information and power transfer," *IEEE Trans. Wireless Commun.*, vol. 12, no. 5, pp. 1989–2001, May 2013.

[8] L. Liu, R. Zhang, and K.-C. Chua, "Wireless information and power transfer: A dynamic power splitting approach," *IEEE Trans. Commun.*, vol. 61, no. 9, pp. 3990–4001, Sep. 2013.

[9] X. Zhou, R. Zhang, and C. K. Ho, "Wireless information and power transfer: Architecture design and rate-energy tradeoff," *IEEE Trans. Commun.*, vol. 61, no. 11, pp. 4754–4767, Nov. 2013.

[10] Z. Xiang and M. Tao, "Robust beamforming for wireless information and power transmission," *IEEE Wireless Commun. Lett.*, vol. 1, no. 4, pp. 3565–3577, Jul. 2014.

[11] Z. Ding, S. M. Perlaza, I. Esnaola, and H. V. Poor, "Power allocation strategies in energy harvesting wireless cooperative networks," *IEEE Trans. Wireless Commun.*, vol. 13, no. 2, pp. 846–860, Feb. 2014.

[12] Z. Ding and H. V. Poor, "Cooperative energy harvesting networks with spatially random users," *IEEE Signal Process. Lett.*, vol. 20, no. 12, pp. 1211–1214, Dec. 2013.

[13] Z. Ding, I. Krikidis, B. Sharif, and H. V. Poor, "Wireless information and power transfer in cooperative networks with spatially random relays," *IEEE Trans. Wireless Commun.*, vol. 13, no. 8, pp. 4440–4453, Aug. 2014.

[14] C. Zhong, H. A. Suraweera, G. Zheng, I. Krikidis, and Z. Zhang, "Wireless information and power transfer with full duplex relaying," *IEEE Trans. Commun.*, vol. 62, no. 10, pp. 3447–3461, Oct. 2014.

[15] G. Zhu, C. Zhong, H. A. Suraweera, G. K. Karagiannidis, Z. Zhang, and T. A. Tsiftsis, "Wireless information and power transfer in relay systems with multiple antennas and interference," *IEEE Trans. Commun.*, vol. 63, no. 4, pp. 1400–1418, Apr. 2015.

[16] M. Mohammadi, B. Chalise, H. A. Suraweera, C. Zhong, G. Zheng, and I. Krikidis, "Throughput analysis and optimization of wireless-powered multiple antenna full-duplex relay systems," *IEEE Trans. Commun.*, vol. 64, no. 4, pp. 1769–1785, Apr. 2016.

[17] H. Liang, C. Zhong, X. Chen, H. A. Suraweera, and Z. Zhang, "Wireless powered dual-hop multi-antenna relaying systems: Impact of CSI and antenna correlation," *IEEE Trans. Wireless Commun.*, vol. 16, no. 4, pp. 2505–2519, Apr. 2017.

[18] H. Liang, C. Zhong, H. A. Suraweera, G. Zheng, and Z. Zhang, "Optimization and analysis of wireless powered multi-antenna cooperative systems," *IEEE Trans. Wireless Commun.*, vol. 16, no. 5, pp. 3267–3281, May 2017.

[19] K. Huang and X. Zhou, "Cutting the last wires for mobile communications by microwave power transfer," *IEEE Commun. Mag.*, vol. 53, no. 6, pp. 86–93, Jun. 2015.

[20] K. Huang and V. K. N. Lau, "Enabling wireless power transfer in cellular networks: Architecture, modeling and deployment," *IEEE Trans. Wireless Commun.*, vol. 13, no. 2, pp. 902–912, Feb. 2014.

[21] Y. Ma, H. Chen, Z. Lin, Y. Li, and B. Vucetic, "Distributed and optimal resource allocation for power beacon-assisted wireless-powered communications," *IEEE Trans. Commun.*, vol. 63, no. 10, pp. 3569–3583, Oct. 2015.

[22] C. Zhong, G. Zheng, Z. Zhang, and G. K. Karagiannidis, "Optimum wirelessly powered relaying," *IEEE Signal Process. Lett.*, vol. 22, no. 10, pp. 1728–1732, Oct. 2015.

[23] S. Luo and K. C. Teh, "Throughput maximization for wireless-powered buffer-aided cooperative relaying systems," *IEEE Trans. Commun.*, vol. 64, no. 6, pp. 2299–2310, Jun. 2016.
[24] C. Zhong, X. Chen, Z. Zhang, and G. K. Karagiannidis, "Wireless-powered communications: Performance analysis and optimization," *IEEE Trans. Commun.*, vol. 63, no. 12, pp. 5178–5190, Dec. 2015.
[25] Y. Zeng and R. Zhang, "Optimized training design for wireless energy transfer," *IEEE Trans. Commun.*, vol. 63, no. 2, pp. 536–550, Feb. 2015.
[26] T. S. Rappaport, *Wireless Communications: Principles and Practice*. Englewood Cliffs, NJ, USA: Prentice-Hall, 2001.
[27] I. Krikidis, S. Sasaki, S. Timotheou, and Z. Ding, "A low complexity antenna switching for joint wireless information and energy transfer in MIMO relay channels," *IEEE Trans. Commun.*, vol. 62, no. 5, pp. 1577–1587, May 2014.
[28] U. Olgun, C. Chen, and J. L. Volakis, "Investigation of rectenna array configurations for enhanced RF power harvesting," *IEEE Antennas Wireless Propag. Lett.*, vol. 10, pp. 262–265, 2011.
[29] H. Lee, K. J. Lee, H. B. Kong, and I. Lee, "Sum-rate maximization for multiuser MIMO wireless powered communication networks," *IEEE Trans. Veh. Technol.*, vol. 65, no. 11, pp. 9420–9424, Nov. 2016.
[30] A. Lozano, A. M. Tulino, and S. Verdú, "High-SNR power offset in multiantenna communication," *IEEE Trans. Inf. Theory*, vol. 51, no. 12, pp. 4134–4151, Dec. 2005.
[31] R. J. Muirhead, *Aspects of Multivariate Statistical Theory*. New York, NY, USA: Wiley, 1982.
[32] I. S. Gradshteyn and I. M. Ryzhik, *Table of Integrals, Series, and Products*, 6th ed. San Diego, CA, USA: Academic, 2000.
[33] A. Lapidoth and S. M. Moser, "Capacity bounds via duality with applications to multiple-antenna systems on flat-fading channels," *IEEE Trans. Inf. Theory*, vol. 49, no. 10, pp. 2426–2467, Oct. 2003.
[34] R. M. Corless, G. H. Gonnet, D. E. G. Hare, D. J. Jeffrey, and D. E. Knuth, "On the Lambert W function," in *Advances in Computational Mathematics*. New York, NY, USA: Springer-Verlag, 1996, pp. 329–359.
[35] S. Verdú, "Spectral efficiency in the wideband regime," *IEEE Trans. Inf. Theory*, vol. 48, no. 6, pp. 1319–1343, Jun. 2002.
[36] A. Lozano, A. M. Tulino, and S. Verdú, "Multiple-antenna capacity in the low-power regime," *IEEE Trans. Info. Theory*, vol. 49, no. 10, pp. 2527–2544, Oct. 2003.
[37] S. Shamai (Shitz) and S. Verdú, "The impact of frequency-flat fading on the spectral efficiency of CDMA," *IEEE Trans. Inf. Theory*, vol. 47, no. 4, pp. 1302–1327, May 2001.
[38] O. Oyman, R. U. Nabar, H. Bolcskei, and A. J. Paulraj, "Characterizing the statistical properties of mutual information in MIMO channels," *IEEE Trans. Signal Process.*, vol. 51, no. 11, pp. 2784–2795, Nov. 2003.
[39] T. M. Cover and J. A. Thomas, *Elements of Information Theory*. New York, NY, USA: Wiley, 1991.
[40] S. Jin, X. Gao, and X. You, "On the Ergodic capacity of rank-1 Ricean-fading MIMO channels," *IEEE Trans. Inf. Theory*, vol. 53, no. 2, pp. 502–517, Feb. 2007.
[41] A. Grant, "Rayleigh fading multi-antenna channels," *EURASIP J. Appl. Signal Process.*, vol. 2002, no. 3, pp. 316–329, Mar. 2002.
[42] H. Wang, L. Chen, and W. Wang, "Enhancing physical layer security through beamforming and noise injection," in *Proc. IEEE WCSP*, Hefei, China, Dec. 2014, pp. 1–6.

Feiran Zhao (S'17) received the B.S. degree in electronic and information engineering from Tianjin Polytechnic University, Tianjin, China, in 2015. He is currently pursuing the Ph.D. degree with the College of Information Science and Electronic Engineering, Zhejiang University. His research interests include wireless-powered communications.

Hai Lin (M'05–SM'12) received the B.E. degree from Shanghai JiaoTong University, China, in 1993, the M.E. degree from the University of the Ryukyus, Nishihara, Japan, in 2000, and the Dr.Eng. degree from Osaka Prefecture University, Japan, in 2005. Since 2000, he has been a Research Associate with the Graduate School of Engineering, Osaka Prefecture University, where he is currently an Associate Professor. His research interests are in signal processing for communications, wireless communications, and statistical signal processing.

Dr. Lin is a member of the IEICE. He served as the Technical Program Committee Member of the IEEE ICC, GLOBECOM, WCNC, and VTC, and the Technical Program Co-Chair at the Wireless Communications Symposium of the IEEE ICC 2011, the Signal Processing for Communications Symposium of the IEEE ICC 2013, and the Wireless Communications Symposium of the IEEE GLOBECOM 2013. He was an Editor of the IEEE TRANSACTIONS ON WIRELESS COMMUNICATIONS, and is currently an Editor of the IEEE TRANSACTIONS ON VEHICULAR TECHNOLOGY.

Caijun Zhong (S'07–M'10–SM'14) received the B.S. degree in information engineering from Xi'an Jiaotong University, Xi'an, China, in 2004, and the M.S. degree in information security and the Ph.D. degree in telecommunications from University College London, London, U.K., in 2006 and 2010, respectively. From 2009 to 2011, he was a Research Fellow with the Institute for Electronics, Communications and Information Technologies, Queen's University Belfast, Belfast, U.K. Since 2011, he has been with Zhejiang University, Hangzhou, China, where he is currently an Associate Professor. His research interests include massive MIMO systems, full-duplex communications, wireless power transfer, and physical layer security.

Dr. Zhong is a recipient of the 2013 IEEE ComSoc Asia–Pacific Outstanding Young Researcher Award. He and his co-authors have been awarded the Best Paper Award at the WCSP in 2013. He is an Editor of the IEEE TRANSACTIONS ON WIRELESS COMMUNICATIONS, the IEEE COMMUNICATIONS LETTERS, *EURASIP Journal on Wireless Communications and Networking*, and the *Journal of Communications and Networks*. He was an Exemplary Reviewer for the IEEE TRANSACTIONS ON COMMUNICATIONS in 2014.

Zoran Hadzi-Velkov (M'97–SM'11) received the Dipl.-Ing. degree (Hons.) in electrical engineering, the Magister Ingenieur degree (Hons.) in communications engineering, and the Ph.D. degree in technical sciences from the Ss. Cyril and Methodius University, Skopje, Macedonia. From 2001 to 2002, he was a Visiting Scholar with the IBM Watson Research Center, New York City, NY, USA. From 2012 to 2014, he was a Visiting Professor with the Institute for Digital Communications, University of Erlangen–Nuremberg, Erlangen, Germany. He is currently a Professor of telecommunications. His research interests include the broad area of wireless communications, with particular emphasis on energy harvesting communications, green communications, and cooperative communications. He received the Alexander von Humboldt Fellowship for experienced researchers in 2012 and the Annual Best Scientist Award from Ss. Cyril and Methodius University in 2014. From 2012 to 2015, he was the Chair of the Macedonian Chapter of the IEEE Communications Society. He has served on the Technical Program Committees of numerous IEEE conferences, including ICC and GLOBECOM. From 2012 to 2016, he served as an Editor of the IEEE COMMUNICATIONS LETTERS.

George K. Karagiannidis (M'96–SM'03–F'14) was born in Pithagorion, Samos Island, Greece. He received the University Diploma and Ph.D. degrees in electrical and computer engineering from the University of Patras, in 1987 and 1999, respectively. From 2000 to 2004, he was a Senior Researcher with the Institute for Space Applications and Remote Sensing, National Observatory of Athens, Greece. In 2004, he joined the Faculty of the Aristotle University of Thessaloniki, Greece, where he is currently a Professor with the Electrical and Computer Engineering Department and the Director of the Digital Telecommunications Systems and Networks Laboratory and also an Honorary Professor with South West Jiaotong University, Chengdu, China.

He has authored or co-authored over 400 technical papers published in scientific journals and presented at international conferences. He has authored the Greek edition of a book on telecommunications systems and has co-authored the book *Advanced Optical Wireless Communications Systems* (Cambridge, 2012). His research interests are in the broad area of digital communications systems and signal processing, with emphasis on wireless communications, optical wireless communications, wireless power transfer and applications, molecular and nanoscale communications, stochastic processes in biology, and wireless security.

Dr. Karagiannidis was the General Chair, the Technical Program Chair, and a member of Technical Program Committees in several IEEE and non-IEEE conferences. He was an Editor of the IEEE TRANSACTIONS ON COMMUNICATIONS, a Senior Editor of the IEEE COMMUNICATIONS LETTERS, an Editor of the *EURASIP Journal of Wireless Communications & Networks* and several times a Guest Editor of the IEEE SELECTED AREAS IN COMMUNICATIONS. From 2012 to 2015, he was the Editor-in-Chief of the IEEE COMMUNICATIONS LETTERS.

He is one of the highly cited authors across all areas of electrical engineering, recognized as Thomson Reuters highly-cited researcher in 2015 and 2016.

Zhaoyang Zhang (M'00) received the Ph.D. degree in communication and information systems from Zhejiang University, Hangzhou, China, in 1998. Since 1998, he has been with the College of Information Science and Electronic Engineering, Zhejiang University, where he became a Full Professor in 2005. He has a wide variety of research interests, including information theory and coding theory, signal processing for communications and in networks, and computation-and-communication theoretic analysis. He was a co-recipient of four international conference best paper/best student paper awards. He is currently serving as an Editor of the IEEE TRANSACTIONS ON COMMUNICATIONS, *IET Communications*, and other international journals. He served as general chair, TPC co-chair, and symposium co-chair for many international conferences and workshops, such ChinaCOM 2008, ICUFN 2011/2012/2013, WCSP 2013, Globecom 2014 Wireless Communications Symposium, and VTC-Fall 2017 Workshop HMWC.